International Journal of Computational and Experimental Science and ENgineering
(IJCESEN)

Vol. 11-No.2 (2025) pp. 3532-3541
http://www.ijcesen.com

ISSN: 2149-9144

Research Article

Multi Spike AMC-Equipped Coaxial Fed Antenna for Gain and Efficiency Enhancement

Padmalatha Lanka*[1,2], S Nagakishore Bhavanam[3], Vasujadevi Midasala[4]

[1]Research Scholar, Acharya Nagarjuna University, Nagarjuna Nagar, Guntur, Andhra Pradesh, 522510, India.
[2]Assistant Professor, ECE department, Seshadri Rao Gudlavalleru Engineering College, Gudlavalleru, Andhra Pradesh, 521356, India
* **Corresponding Author Email:** plgec07@gmail.com - **ORCID:** 0000-0002-5247-785X

[3]Associate Professor, Department of Computer Science and Engineering, Mangalayatan University Jabalpur (MUJ), Madhya Pradesh, India.
Email: plgec07@gmail.com - **ORCID:** 0000-0002-5247-785Y

[4]Associate Professor, Department of Computer Science and Engineering, Mangalayatan University Jabalpur (MUJ), Madhya Pradesh, India.
Email: plgec07@gmail.com - **ORCID:** 0000-0002-5247-785Z

Article Info:

DOI: 10.22399/ijcesen.927
Received : 30 November 2024
Accepted : 22 February 2025

Keywords:

AMC,
Coaxial Fed,
Gain,
Mutli Spike

Abstract:

A low-profile patch antenna based on artificial magnetic conductors (AMC) is being developed for microwave applications. In this article, we proposed an antenna with a DGS (defective ground structure) structure and an array of AMC to improve the antenna's radiation performance. There is an air gap of 10 mm present between proposed antenna and AMC surface. The proposed models operate at two operating frequencies with S11 values of less than - 10 dB in the 4.20-4.28 and 4.86-5.0 GHz bands, respectively. The antenna achieved a gain of 10.1 dBi at 4.25 GHz and 9.54 dBi at 4.91 GHz, respectively. A significant degree of agreement exists between the antenna's simulated and measured parameters.

1. Introduction

Over the last few decades, the adoption of microstrip patch antennas for any type of microwave applications has had a tremendous impact on wireless communications. Traditional patch antennas have various drawbacks in their radiation parameters. There are several approaches for enhancing the efficiency of antennas. In recent years, there has been a proliferation of cutting-edge methodologies and models for antenna and AMC design [1-4]. different kinds of antennas like wearable antennas, planer antennas, microstrip antennas, and monopole antennas have been proposed for microwave applications [5, 6].
Unfortunately, the fact that these antennas are limited to a single frequency band means that designing a single antenna will not result in gain enhancement. A dual-band, dual-polarized antenna for WLANs was developed in [7] and placed on an AMC reflector. A dual-band antenna with independently controlled radiating elements could have gained up to 3.1 dBi, as proposed in [8]. The antennas described in references [9] and [10] are complexly built and have gains greater than 10 dB, which limits their practical use. so, the goal of developing a wideband microstrip antenna that is compact, light, inexpensive remains unfulfilled. A dual- band antenna such as that described in [11] is suitable for long-distance communications because it has a high gain, can be dual circularly polarized, and has minimal backward radiation.
Unfortunately, the fact that these antennas are limited to a single frequency band means that designing a single antenna will not result in gain enhancement. A dual-band, dual-polarized antenna for WLANs was developed in [7] and placed on an AMC reflector. A dual-band antenna with independently controlled radiating elements could have gained up to 3.1 dBi, as proposed in [8]. The antennas described in references [9] and [10] are complexly built and have gains greater than 10 dB,

which limits their practical use. so, the goal of developing a wideband microstrip antenna that is compact, light, inexpensive remains unfulfilled. A dual- band antenna such as that described in [11] is suitable for long-distance communications because it has a high gain, can be dual circularly polarized, and has minimal backward radiation.

Unfortunately, the fact that these antennas are limited to a single frequency band means that designing a single antenna will not result in gain enhancement. A dual-band, dual-polarized antenna for WLANs was developed in [7] and placed on an AMC reflector. A dual-band antenna with independently controlled radiating elements could have gained up to 3.1 dBi, as proposed in [8]. The antennas described in references [9] and [10] are complexly built and have gains greater than 10 dB, which limits their practical use. so, the goal of developing a wideband microstrip antenna that is compact, light, inexpensive remains unfulfilled. A dual- band antenna such as that described in [11] is suitable for long-distance communications because it has a high gain, can be dual circularly polarized, and has minimal backward radiation.

2. 2. Design description of proposed antenna

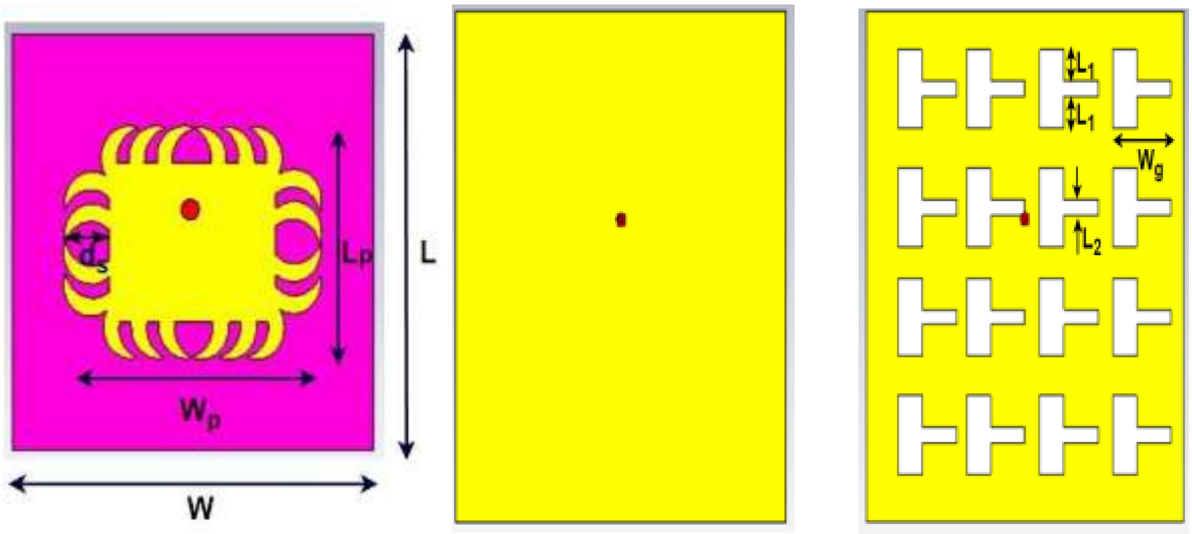

(a) **(b)** **(c)**

Figure 1. *Proposed spike shaped patch antenna (a) Front side (b) Back side with full ground and (c) Backside ground with DGS (defective ground structure)*

Table. 1. *Proposed antenna dimensions*

Parameter	Dimension(mm)
L	10.0
W	10.0
Lp	3.75
Wp	4.96
L1	0.4
L2	0.2
Wg	2.0
ds	1.0
ts	0.8

As illustrated in figure 1, the spike shaped patch antenna contains spikes around the patch antenna and the radius of any spike is chosen as 0.5mm. A copper material is chosen as a conductive material for both ground and the spike shaped patch. FR-4 material with a thickness of 0.8mm is chosen as a dielectric substrate for the antenna. S11 (dB) plot for the proposed antenna covered with full copper for ground layer is shown in figure 2 and in order to achieve two resonant frequency bands, the ground plane is equipped with T-shaped slots, as illustrated in figure 3.

3. Results Description

From the figure 2, it can be noted that with numerical simulation tool like CST studio, the antenna is resonating at 4.58GHz frequency with S11 of -12.51dB, whereas with measurement the antenna structure is resonating at same frequency with reflection coefficient (S11) of - 11.70dB. Here red colour indicates simulated S11 and black coloured dotted line indicates measured S11.Here, we obtained less S11 value and antenna is operating at only single operating frequency band. So, to improve the number of resonating frequency bands, we have taken concept of defective ground structure (DGS). Here, a T-shaped slots are arranged for the ground plane. As a result the antenna is operating at two frequencies in C-band. The simulated S11 plot is clearly represented by the solid red curve in Figure 3, whereas the measured S11 plot is denoted by the dot-marked black curve. The simulated S11 parameter exhibits resonance at 4.25 GHz and 4.91 GHz with magnitudes of -19.93 dB and -29.79 dB, respectively. In contrast, the measured S11 parameter exhibits resonance at the same frequencies with magnitudes of -16.05 dB and 19.73 dB respectively

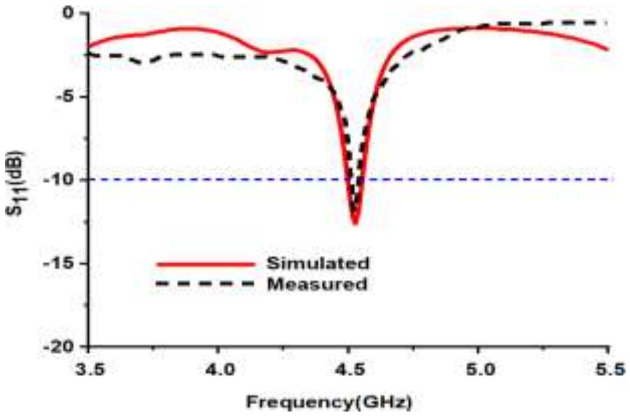

***Figure 2**. S11 (dB) for the proposed spike shaped patch antenna without DGS*

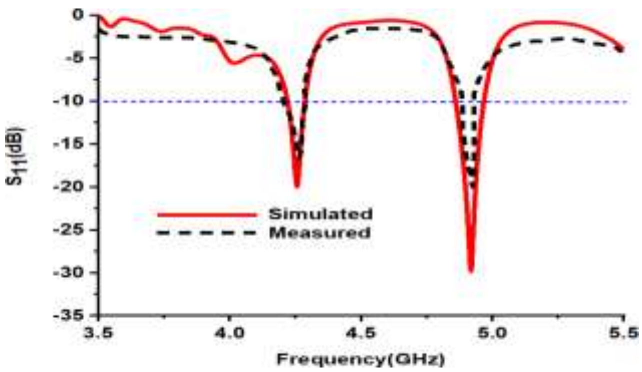

***Figure 3**. S11 (dB) for the proposed spike shaped patch antenna with DGS*

From the figure 2, it can be noted that with numerical simulation tool like CST studio, the antenna is resonating at 4.58GHz frequency with S11 of - 12.51dB, whereas with measurement the antenna structure is resonating at same frequency with reflection coefficient (S11) of - 11.70dB. Here red colour indicates simulated S11 and black coloured dotted line indicates measured S11.Here, we obtained less S11 value and antenna is operating at only single operating frequency band. So, to improve the number of resonating frequency bands, we have taken concept of defective ground structure (DGS). Here, a T-shaped slots are arranged for the ground plane. As a result the antenna is operating at two frequencies in C-band. The simulated S11 plot is clearly represented by the solid red curve in Figure 3, whereas the measured S11 plot is denoted by the dot-marked black curve. The simulated S11 parameter exhibits resonance at 4.25 GHz and 4.91 GHz with magnitudes of -19.93 dB and -29.79 dB, respectively. In contrast, the measured S11 parameter exhibits resonance at the same frequencies with magnitudes of -16.05 dB and 19.73 dB respectively.

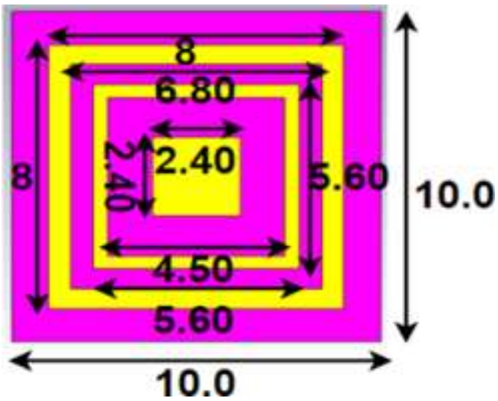

***Figure 4.** Unitcell structure of the proposed AMC surface*

The obtained peak gains for the proposed antenna with DGS structure alone achieved a maximum peak gain of 3.5dBi within the frequency bands from (4.20-4.28) GHz and (4.86- 5.0) GHz. So, to enhance the performance of the proposed antenna, we have proposed an AMC (artificial magnetic conductor) layer for improving the antenna's performance. The proposed AMC layer's unitcell with dimensions for each and every element present on the unit cell is given in figure 4. From the figure 4, we can note that the proposed unit cell contains two square typed rings and a square typed patch and the unit cell dimension is chosen as 10x 10 mm2 When an AMC layer is arranged at the bottom side of the antenna as shown in figure 5(b), the obtained S11 plot is shown in figure 8. The fabricated model and its measurement setup is shown in figure 6 and 7 respectively.

The obtained peak gains for the proposed antenna with DGS structure alone achieved a maximum peak gain of 3.5dBi within the frequency bands from (4.20-4.28) GHz and (4.86- 5.0) GHz. So, to enhance the performance of the proposed antenna, we have proposed an AMC (artificial magnetic conductor) layer for improving the antenna's performance. The proposed AMC layer's unitcell with dimensions for each and every element present on the unit cell is given in figure 4. From the figure 4, we can note that the proposed unit cell contains two square typed rings and a square typed patch and the unit cell dimension is chosen as 10x 10 mm2

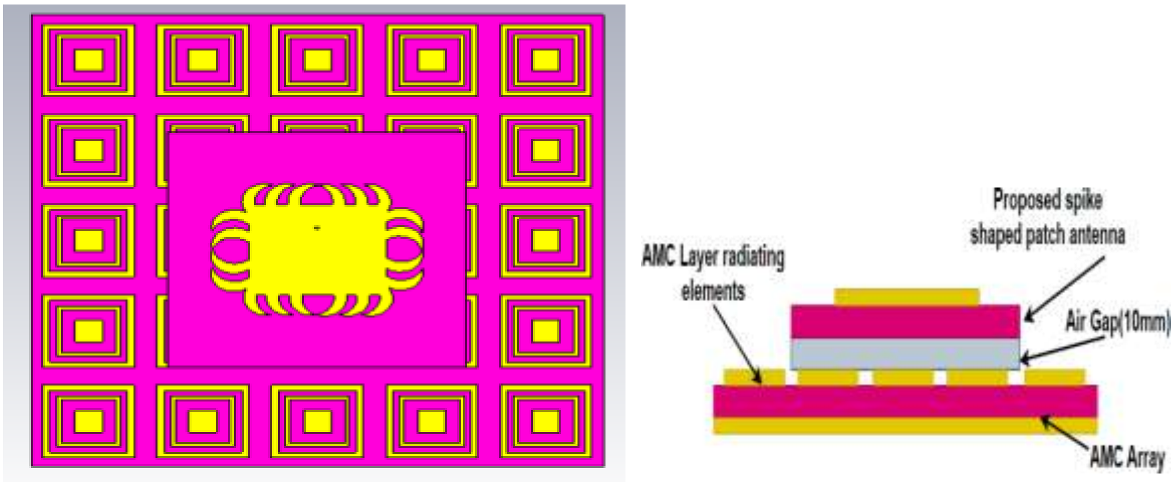

(a) (b)

***Figure 5**. Proposed antenna with an AMC surface (a) Top view and (b) side views*

(a) *(b)*

***Figure 6.** Proposed fabricated models (a) antenna (b) AMC surface*

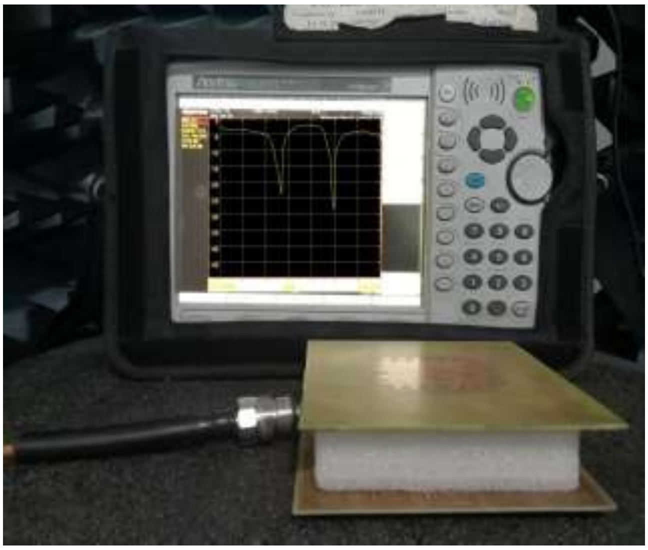

***Figure 7**. Measurement setup of antenna and AMC*

When an AMC layer is arranged at the bottom side of the antenna as shown in figure 5(b), the obtained S11 plot is shown in figure 8. The fabricated model and its measurement setup is shown in figure 6 and 7 respectively.

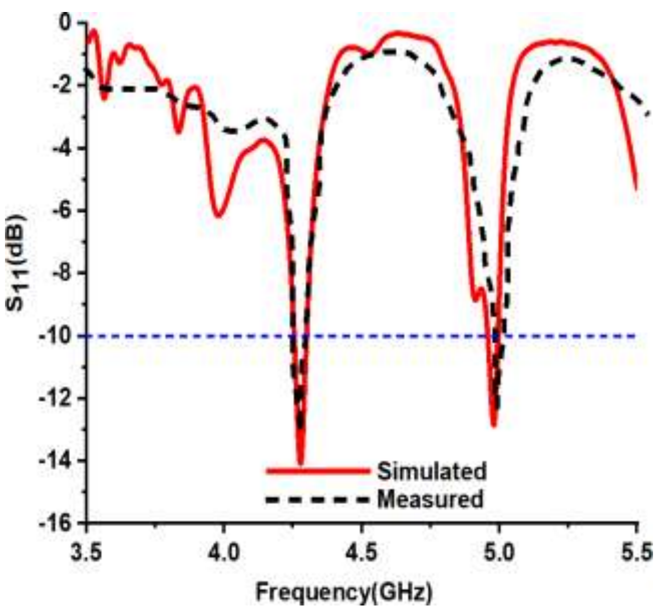

***Figure 8**. S11(dB) for the proposed antenna with an AMC layer*

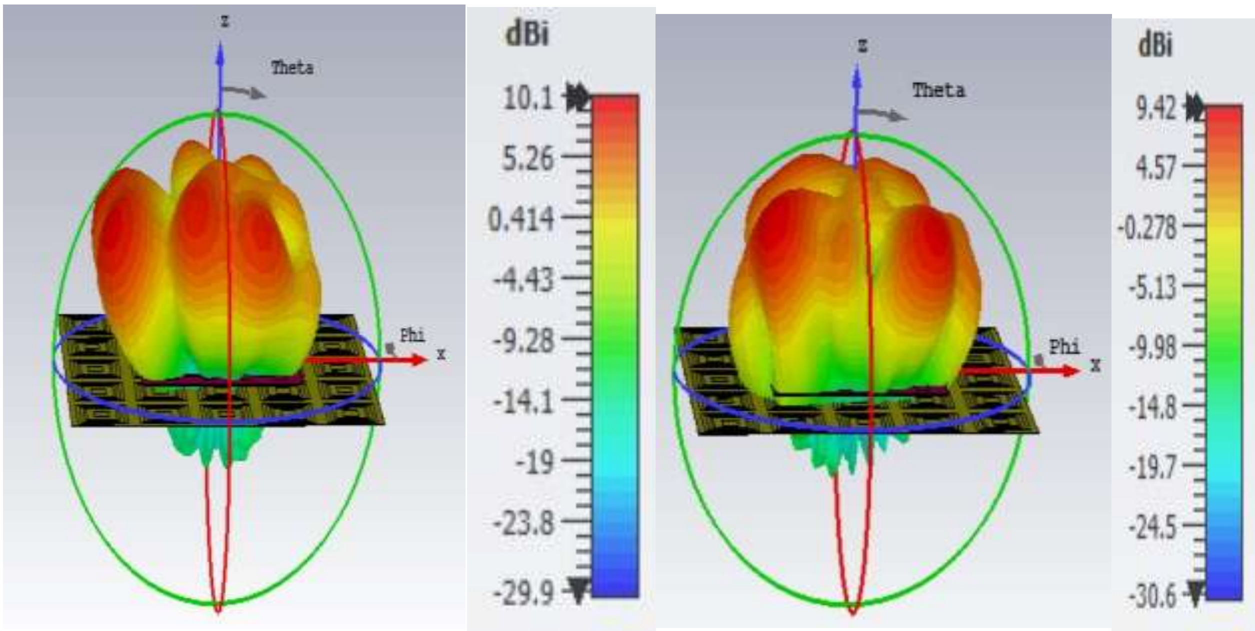

(a) (b)

Figure 9. *3D radiation patterns of the antenna with DGS and using an AMC layer at (a) 4.25 GHz and (b) 4.91GHz frequencies*

In figure 5, the yellow colour indicates conductive part and magenta colour indicates dielectric material for both antenna and AMC layers. Based on the data presented in Figure 8, it is evident that the simulated S11 parameter exhibits resonance at 4.27 GHz and 4.98 GHz with magnitudes of -14.07 dB and -12.83 dB, respectively, caused by the AMC surface and with measurementation, S11 exhibits resonance at the same frequencies with magnitudes of 12.58 dB and -12.15 dB respectively. 3D radiation patterns of the antenna with DGS and using an AMC layer at 4.25 GHz and 4.91GHz frequencies are shown in figure 9.

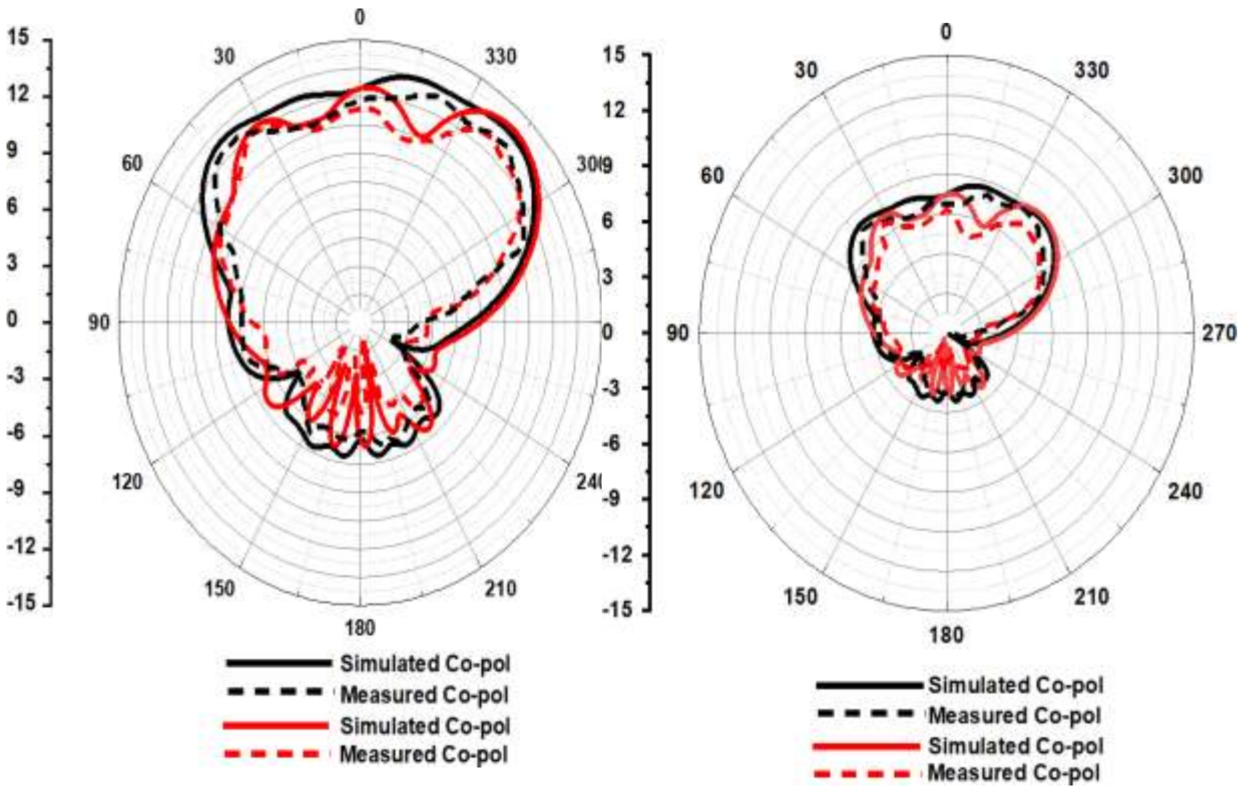

(a) (b)

Figure 10. *Radiation patterns of the antenna with an AMC layer at 4.25 GHz frequency in both (a) E- and (b) H-planes,*

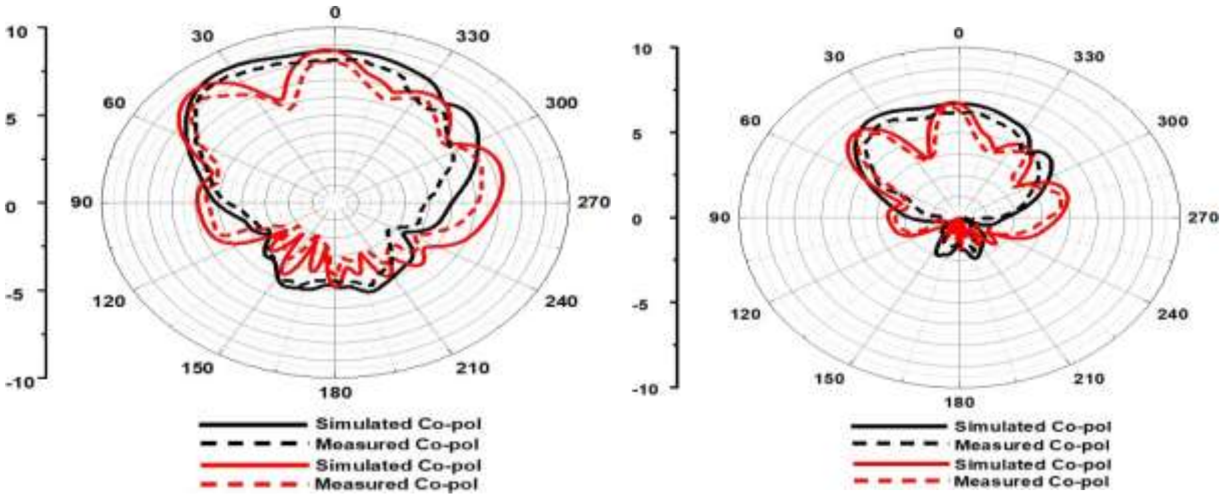

(a) *(b)*

Figure 11. *Radiation patterns of the antenna with an AMC layer at 4.91 GHz frequency in both (a) E- and (b) H-planes,*

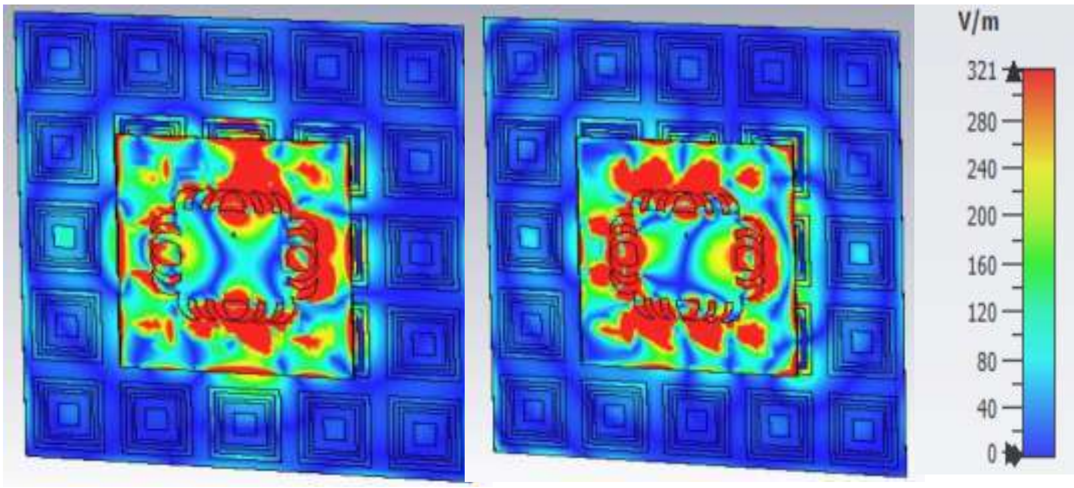

(a) *(b)* *(c)*

Figure 12. *E-distribution of the proposed spike shaped patch antenna with an AMC layer at (a) 4.25GHz (b) 4.91GHz frequencies with (c) scale*

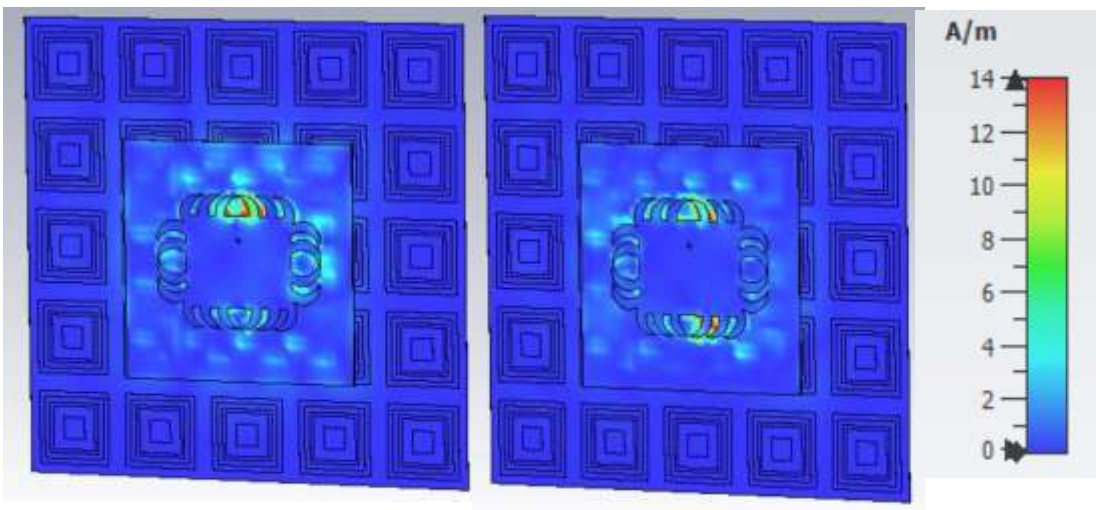

(a) *(b)* *(c)*

Figure 13. *H-distribution of the proposed spike shaped patch antenna with an AMC layer at (a) 4.25GHz (b) 4.91GHz frequencies with (c) scale*

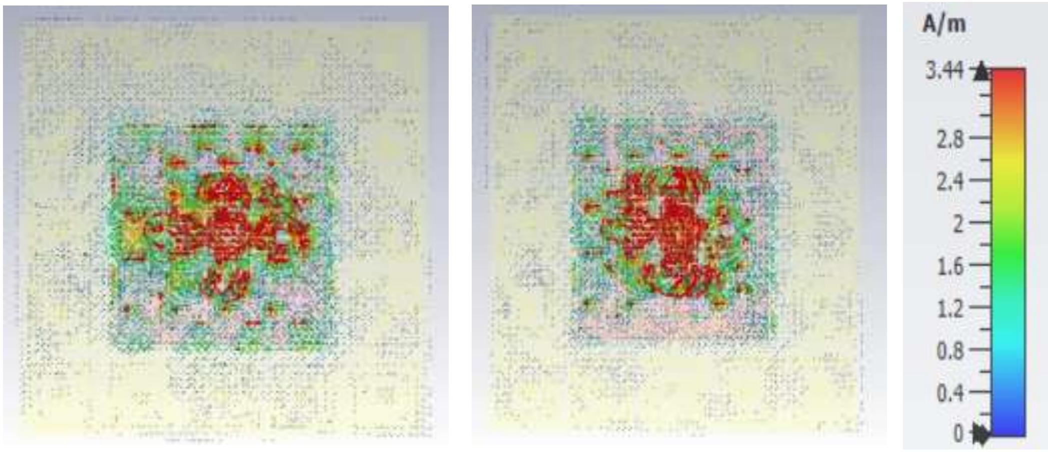

(a) *(b)* *(c)*

Figure 14. *Surface current distributions of the proposed spike shaped patch antenna with an AMC layer at (a) 4.25GHz (b) 4.91GHz frequencies with (c) scale*

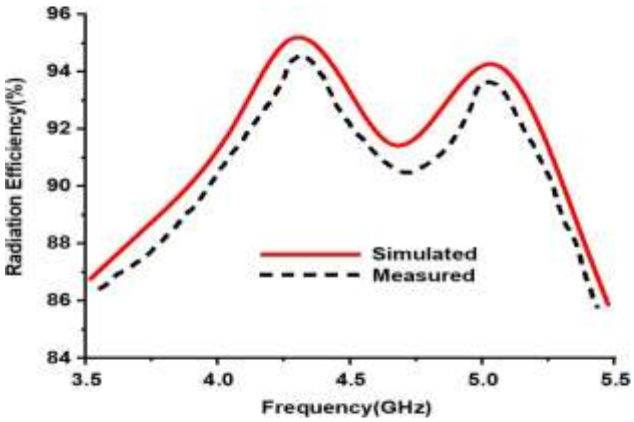

Figure 15. *Radiation efficiency versus frequency plot of the proposed antenna with an AMC layer*

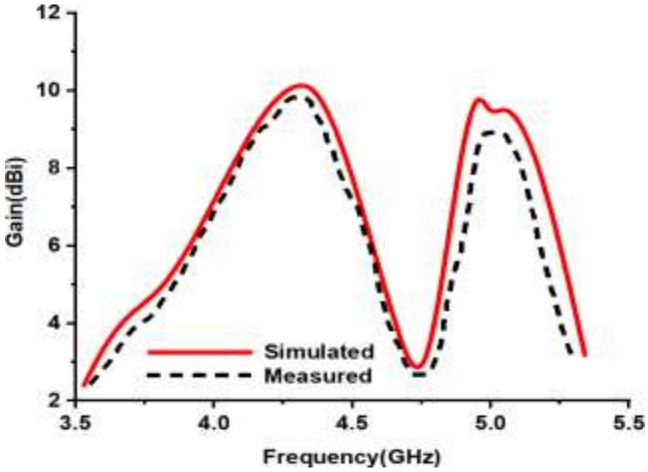

Figure 16. *Gain versus frequency plot of the proposed antenna with an AMC layer*

For a better understanding of the performance enhancement of combined antenna with AMC, rather than the single antenna alone with DGS, the radiation patterns for the single antenna and antenna + AMC combination at a lower frequency 4.25 GHz and the upper frequency 4.91 GHz both in E-plane and H-planes with AMC is explained clearly in figure 10 and figure 11 for both resonant frequencies respectively. From figure 10 and figure 11 we can observe that there is small amount of back radiation due to AMC structure. From figure 12, it can be noted that a maximum electric field can be observed on gaps present between the spikes at both resonant frequencies and a minimum H-field can be observed at both resonant frequencies as shown in figure 11. Similarly, Surface current distributions of the proposed spike shaped patch antenna with an AMC layer is shown in figure 14 at both resonant frequencies. Gain and efficiency plots for the proposed spike shaped patch antenna with an AMC layer is shown in figure 15 and figure 16 respectively. From the figure 15, it can be noted that the red-coloured solid line represents simulated plot and black coloured dotted line represents measured plot. The simulated obtained gains of the DGS patch antenna with AMC were 10.1 and 9.54 dBi at 4.25GHz and 4.91GHz frequencies respectively, whereas the measured gains of the DGS patch antenna with AMC were 9.83 and 9.35 dBi at 4.25GHz and 4.91GHz frequencies respectively.

To demonstrate the entire spike-shaped antenna, we use an equivalent circuit model and test it using the ADS tool. Figure 17 shows that inductor L3 represents the whole radiating patch, while capacitor C3 represents the space between any two spikes. In the same way, an inductor L4 represents the complete ground plane of the antenna, and the gap present in the ground plane like a T-shape can be indicated by C4. To replicate the S-parameter response depicted in Figure 18, the RF input is matched to a 50-ohm impedance to produce the expected outcome. To achieve the desired return loss (S11) response, the initial and final frequencies are configured to 3.5 GHz and 5.5 GHz, by employing a 50 MHz frequency increment respectively. Figure 16 shows that the X-axis specifies a frequency range of

3.5 to 5.5 GHz, and the Y-axis displays the chosen S11 (dB). Table 2 shows the results of comparing this work to the current state of the art. As can be seen from the table, the proposed antenna structure achieved maximum peak gain while maintaining a small dimension of 50.0 x 50.0 mm2.

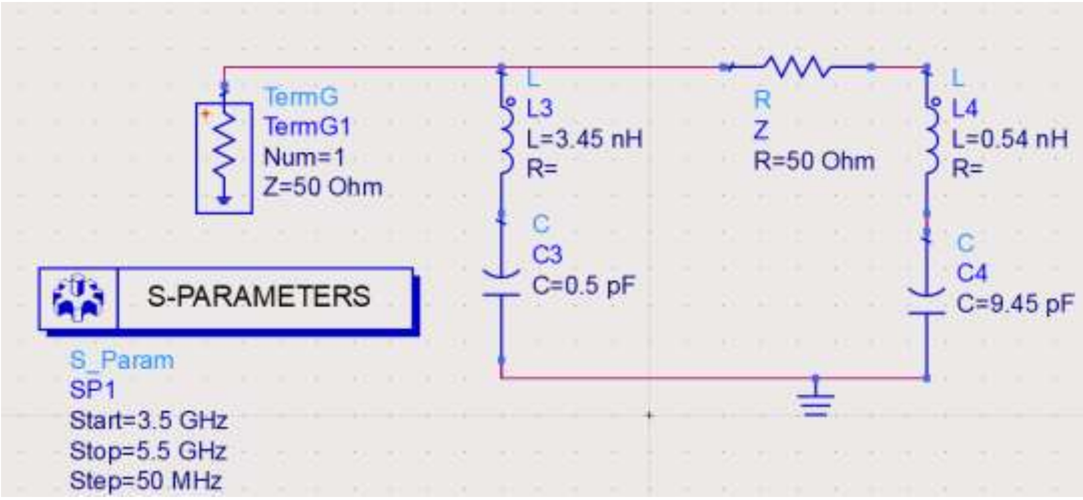

Figure 17. *Equivalent circuit model of the proposed antenna with an AMC layer*

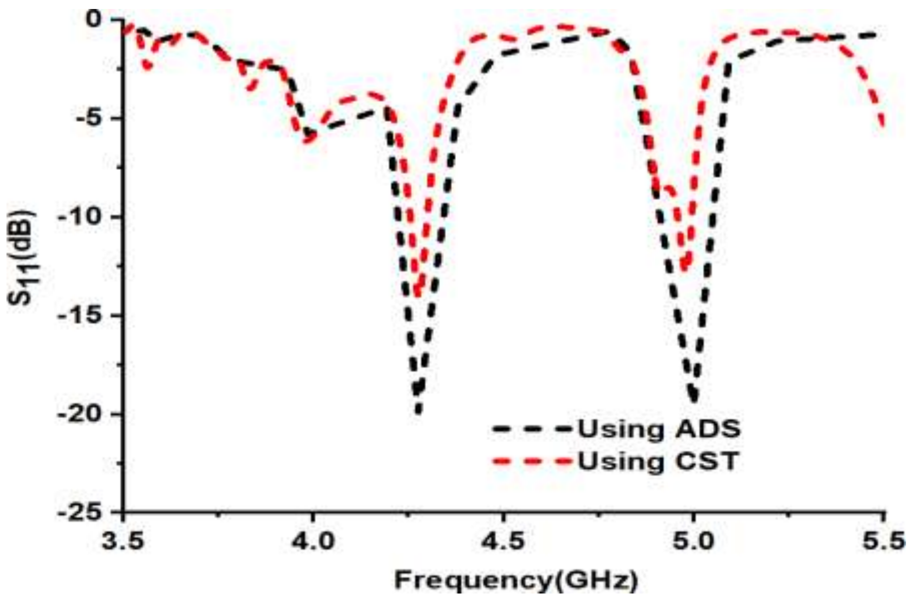

Figure 18. *S_{11} (dB) plot for the of the proposed antenna with DGS*

To demonstrate the entire spike-shaped antenna, we use an equivalent circuit model and test it using the ADS tool. Figure 17 shows that inductor L3 represents the whole radiating patch, while capacitor C3 represents the space between any two spikes. In the same way, an inductor L4 represents the complete ground plane of the antenna, and the gap present in the ground plane like a T-shape can be indicated by C4. To replicate the S-parameter response depicted in Figure 18, the RF input is matched to a 50-ohm impedance to produce the expected outcome. To achieve the desired return loss (S11) response, the initial and final frequencies are configured to 3.5 GHz and 5.5 GHz, by employing a 50 MHz frequency increment respectively. Figure 16 shows that the X-axis specifies a frequency range of 3.5 to 5.5 GHz, and the Y-axis displays the chosen S11 (dB). Table 2 shows the results of comparing this work to the current state of the art. As can be seen from the table, the proposed antenna structure achieved maximum peak gain while maintaining a small dimension of 50.0 x 50.0 mm^2.

Table 2.*Comparision* table for the proposed work with existing

Ref. No.	Substrate material	Operating Frequency band	Maximum obtained peak gain (dBi)	Antenna size (mm^2)
[12]	Rogers	S	6.40	83.0 x 89.0
[13]	Rogers	S	9.40	36.0 x 18.0
[14]	PDMS	S	5.20	21.0 x 21.0
[15]	Rogers	S	6.20	39.0 x 30.0
[16]	Polyimide	S and C	6.90	61.5 x 61.5
[17]	FR4	S and C	8.20	29.2 x 29.2
[18]	Polymide	S and C	7.87	49.0 x 29.0
[19]	FR-4	C and X	17	20 x 12
[20]	FR-4	S, C, X and Ku	7.18	40.0 x 44.0
[21]	FR-4	S, C, X and Ku	4.8	50.0 x 50.0
[22]	FR-4	S and L	6.8	70.0 x 31.0
[23]	RT-Duroid	S	4.9	41.52 x 35.9
[24]	FR-4	S, C, X and Ku	5.44	20.0 x 20.0
[25]	FR-4	S and C	5.86	30.0 x 17.0
[26]	FR-4	S and C	4	50.0 x 52.0
This work	FR4	C	10.1	50.0 x 50.0

4. Conclusions

We have designed, fabricated and tested a low-profile, dual-band, small size antenna provided by AMC. Here an AMC is employed to improve the antenna's performance and to limit backward radiation. The antenna and AMC surfaces are made of 0.8 mm thick FR4 substrate. The antenna has a total dimension of 10*10*0.8 mm3. The antenna was supported by a variety of AMC array sizes to improve its performance. Inside the bands, the antenna gain was determined to be 10.1 and 9.42 dBi, respectively and radiation parameters of the antenna with and without AMC is verified. The electric, magnetic and surface current distribution of the antenna with AMC layer is verified and hence the proposed antenna with AMC structure is very much useful for wireless and other microwave based applications.

Author Statements:

- **Ethical approval:** The conducted research is not related to either human or animal use.
- **Conflict of interest:** The authors declare that they have no known competing financial interests or personal relationships that could have appeared to influence the work reported in this paper

- **Acknowledgement:** The authors declare that they have nobody or no-company to acknowledge.

- **Author contributions:** The authors declare that they have equal right on this paper.

- **Funding information:** The authors declare that there is no funding to be acknowledged.

- **Data availability statement:** The data that support the findings of this study are available on request from the corresponding author. The data are not publicly available due to privacy or ethical restrictions

References

[1] Contopanagos, H.F.A. (2020). broadband polarized artificial magnetic conductor metasurface. *Journal of Electromagnetic Waves and Applications*, 34(14); 1823-1841

[2] Wang, Shuqi, & Huan Gao. (2022). A dual-band wearable conformal antenna based on artificial magnetic conductor. *International Journal of Antennas and Propagation, 2022; 9970477*

[3] Pathan, Tarannum U. & Bhagwat Kakde. (2022). A Compact Circular Polarized MIMO Fabric Antenna with AMC Backing for WBAN Applications. *Advanced Electromagnetics*, 11(3); 26-33.

[4] Chaouche, Youcef Braham, Mourad Nedil, Ismail Ben Mabrouk & Omar M. Ramahi. (2022). A wearable circularly polarized antenna backed by AMC reflector for WBAN communications. *IEEE Access*, 10; 12838-12852.

[5] Abbas, Mohammad Hussain, Shamsher Singh, Ankit Sharma &Deepak Gangwar. (2023). Low- profile high gain circularly polarized CRLH transmission line inspired antenna with artificial magnetic conductor for

wearable applications. *International Journal of Microwave and Wireless Technologies,* 15 (7); 1223-1232.

[6] Chen, Yujun, Xiongying Liu, Yi Fan, & Hongcai Yang. (2022). Wearable wideband circularly polarized array antenna for off-body applications. *IEEE Antennas and Wireless Propagation Letter,s* 21(5); 1051-1055.

[7] Lin, Chia-Hsien, Kazuyuki Saito, Masaharu Takahashi, & Koichi Ito. (2012): A compact planar inverted-F antenna for 2.45 GHz on-body communications. *IEEE transactions on antennas and propagation,* 60 (9); 4422-4426.

[8] Paracha, Kashif Nisar, Sharul Kamal Abdul Rahim, Ping Jack Soh, Muhammad Ramlee Kamarudin, Kim-Geok Tan, Yew Chiong Lo, & Mohammad Tariqul Islam. (2019). A low profile, dual-band, dual polarized antenna for indoor/outdoor wearable application. *IEEE Access,* 7; 33277-33288

[9] Yang, Xujun, Yuan Ji, Lei Ge, Xierong Zeng, Yongle Wu,&Yuanan L.iu. (2020). A dual-band radiation-differentiated patch antenna for future wireless scenes. *IEEE Antennas and Wireless Propagation Letters,* 19 (6); 1007-1011

[10] Jagtap, Shishir, Anjali Chaudhari, Nayana Chaskar, Shilpa Kharche & Rajiv K. Gupta. (2018). A wideband microstrip array design using RIS and PRS layers. *IEEE Antennas and Wireless Propagation Letters,* 17(3); 509-512

[11] Gao, Guo-Ping, Chen Yang, Bin Hu, Rui-Feng Zhang, & Shao-Fei Wang. (2018). A wearable PIFA with an all-textile metasurface for 5 GHz WBAN applications. *IEEE antennas and wireless propagation letters,* 18(2); 288-292

[12] Saeed, S. M., C. A. Balanis, C. R. Birtcher, A. C. Durgun, & H. N. Shaman, (2017). Wearable flexible reconfigurable antenna integrated with artificial magnetic conductor. *IEEE Antennas and Wireless Propagation Letter,* 16; 2396–2399

[13] El Atrash, M., M. A. Abdalla, & H. M. Elhennawy. (2019). A wearable dual-band low profiles high gain low SAR antenna AMC-backed for WBAN applications. *IEEE Transactions on Antennas and Propagation,* 67(10); 6378–6388

[14] Jiang, Z. H., Z. Cui, T. Yue, Y. Zhu, & D. H. Werner. (2017). Compact, highly efficient, and fully flexible circularly polarized antenna enabled by silver nanowires for wireless body-area network. *IEEE Transactions on Biomedical Circuits and Systems,* 11 (4); 920–932

[15] Jiang, Z. H., D. E. Brocker, P. E. Sieber, & D. H. Werner(2014). A compact, low-profile metasurface enabled antenna for wearable medical body area network devices. *IEEE Transactions on Antennas and Propagation,* 62 (8); 4021–4030,

[16] Wang, S. & H. Gao. (2022). A dual-band wearable conformal antenna based on artificial magnetic conductor. *International Journal of Antennas and Propagation,* 2022; 9970477

[17] Liu, Q., H. Liu, W. He, & S. He. (2020). A low-profile dual-band dual-polarized antenna with an AMC reflector for 5G communications. *IEEE Access,* 8; 24072–24080.

[18] Prasad, Nagandla, Pokkunuri Pardhasaradhi, Tanvir Islam, Sudipta Das, & Mohammed El Ghzaoui.(2023). Radiation Performance Improvement of a Staircase Shaped Dual Band Printed Antenna with a Frequency Selective Surface (FSS) for Wireless Communication Applications. *Progress In Electromagnetics Research* C 137 (2023); 53-64

[19] Deepak, Bandhakavi S., Badisa Anil Babu, & Kosuru Sri Rama Murthy. (20219. A Circularly Polarized Semi-Symmetric Curvature Slot Fractal Antenna for Gain Enhancement. *Journal of Engineering Science & Technology Review* 14 (3)

[20] Kishore, M. Purna, SS Mohan Reddy. (2019). Metamaterial inspired gain enhanced elliptical curved CPW fed multiband antenna for medical and wireless communication applications. *Biomedical and Pharmacology Journal* 12 (2); 729-737

[21]Aradhyula, Raghavaraju, TV Rama Krishna,. (2019]. Electromagnetic bandgap structured CPW fed circular monopole antenna with bandwidth enhancement for wideband applications. *Int. J. Innovative Technol. Exploring Eng* 8(10); 879-882.

22. Najumunnisa, Md, Ambadapudi Srinivasa Chandrasekhara Sastry, Sudipta Das, Niamat Hussain, Syed Samser Ali, and Muhammad Aslam. (2022).A Metamaterial Inspired AMC Backed Dual Band Antenna for ISM and RFID Applications. Sensors 22 (20); 8065.

[23] Madhav, B. T. P., D. Naga Vaishnavi, G. Vanaja, G. Jayasree, & S. Mounika. (2015). Design and analysis of metamaterial antenna with EBG loading. Far East Journal of Electronics and Communications 14(2); 127-136.

[24] Madhav, B. T. P., Mounika Sanikommu, M. N. V. S. Pranoop, KSN Manikanta Chandra Bose, and B. Sriram Kumar. CPW fed antenna for wideband applications based on tapered step ground and EBG structure. *Indian Journal of Science and Technology* 8(S9); 119- 27.

[25] Tilak, G. B. G., Sarat K. Kotamraju, K. Ch Sri Kavya, & M. Venkateswara Rao. (2020). Dual sensed high gain heart shaped monopole antenna with planar artificial magnetic conductor. *Journal of Engineering Science and Technology* 15(3); 1952-1971.

[26] Das, Priyanka, Dhulipalla Venkata Rao. (2023). A metasurface integrated shared aperture antenna for Sub-6 GHz applications. *Engineering Research Express* 5(3), 035030.